WIND FIELDS RETRIEVED FROM SAR IN COMPARISON TO NUMERICAL MODELS

Jochen Horstmann[1], Wolfgang Koch[1], and Susanne Lehner[2]

[1]GKSS Research Center, Max-Planck-Str., D-21502 Geesthacht,
Tel. +49 4152 87 1567, Fax: +49 4152 87 1565
[2]Deutsches Zentrum für Luft und Raumfahrt, D-Wessling,
Tel. +49 8153 28 2828, Fax: +49 8153 28 2895

ABSTRACT

An algorithm is introduced, which is designed to retrieve high-resolution wind fields from C-band synthetic aperture radar (SAR) operating at both vertical and horizontal polarization. The wind directions are extracted from wind-induced streaks, which are approximately in line with the mean wind direction near to the ocean surface. Wind speeds are derived from the normalized radar cross section (NRCS) and image geometry of the calibrated SAR images, together with the local wind direction retrieved from the image. Therefore the semi empirical C-band model CMOD4, which describes the dependency of the NRCS on wind and image geometry, is used. CMOD4 was originally developed for the scatterometer of the European remote sensing satellites ERS-1 and 2 operating at C-band with vertical polarization. Consequently CMOD4 requires modification for horizontal polarization, which is performed by considering the polarization ratio. To verify the algorithm, wind fields were computed from 200 ERS SAR and 20 RADARSAT-1 ScanSAR images and compared to co-located results from the numerical model REMO and HIRLAM. In addition three weeks of ERS-2 SAR wave mode data were processed to single look complex SAR images, representing a total of 34000 SAR images of size 5 km x 10 km, which are available on a global basis every 200 km along the satellite track. From these images wind speeds are retrieved using a Neural Network, which parameterises the dependency of SAR-derived intensity on ocean surface wind. The SAR derived winds are compared to co-located winds from the ERS-2 SCAT and the model results of the European Center for Medium-range Weather Forecast (ECMWF).

1. Introduction

Since the launch of the European remote sensing satellites ERS-l and ERS-2, and the Canadian satellite RADARSAT-1, synthetic aperture radar (SAR) images have been acquired over the oceans on a continuous basis. Their independence on daylight and all-weather capability together with their high resolution and large spatial coverage make them a valuable tool, especially in coastal areas, for measuring geophysical parameters such as ocean surface winds, waves, and sea ice. Both SARs operate in the C-band (5.3 GHz) at moderate incidence angles between 20° and 50°. For this electromagnetic wavelength and range of incidence angles the backscatter of the ocean surface is primarily caused by the small-scale surface roughness, which is strongly influenced by the local ocean wind field and therefore allows the backscatter to be related to the wind.

Much effort has been undertaken to develop algorithms for derivation of wind vectors from SAR images. The wind directions can be retrieved from the direction of wind-induced streaks, which are approximately in line with the mean wind direction. The direction of these streaks can either be retrieved by using spectral methods (Gerling, 1986; Vachon and Dobson, 1996; Lehner et al., 1998) or in the spatial domain by a method based on derivation of local gradients (Horstmann et al., 2002, Koch, 2002). The wind speed is derived from the normalized radar cross section (NRCS), which is retrieved from the SAR data, using semi empirical C-band models for vertical (VV) polarization (Vachon and Dobson, 1996; Lehner et al., 1998; Horstmann et al., 2000a). In case of horizontal (HH)

polarization these models have been extended to HH polarization (Horstmann et al., 2000a, 2000b; Thompson and Beal, 2000).

In this paper an algorithm for wind field retrieval from SAR, operating at C-band, is introduced and its application is demonstrated using ERS-1, ERS-2 and RADARSAT-1 SAR imagery. In contrast to previously used wind direction retrieval algorithms, which are based on filtering in the spectral domain, here they are retrieved in the spatial domain. This method allows to retrieve directional information at the coasts and has the potential to suppress wind errors introduced by local sea surface features not due to the wind, e.g., sea ice. In addition to the wind speed retrieval method based on the C-band models, which are dependent on accurate radiometric calibration of the NRCS, a method based on Neural Networks (NN) is applied to an global set of 34310 uncalibrated single look complex ERS-2 SAR wave mode imagettes.

2. Utilized data

The European remote sensing satellite ERS-1 and ERS-2 are equipped with a SAR and a SCAT combined in the active microwave instrument (AMI), which operates with a frequency of 5.3 GHz (C-band) at linear vertical (VV) polarization. The AMI can be operated in the SAR image mode and interleaved mode consisting of the SAR wave mode and SCAT. In the SAR image mode 100 km x 100 km ocean surface can be imaged with a resolution of ~30 m. The SAR data are radiometricaly calibrated for NRCS having a nominal radiometric accuracy of ±0.5 dB. In the SAR wave mode 10 km x 5 km imagettes are acquired at a nominal incidence angle of 23° with a spatial resolution of ~30 m every 200 km along the orbit. These data are available on a continuous basis and have to be processed to SAR single look complex (SLC) imagettes, which are not available as a ERS standard product, but are now available from the advanced SAR (ASAR) aboard the European environmental satellite (ENVISAT). To prepare and validate algorithms for the ENVISAT ASAR, the German Aerospace Center processed 27 days of uncalibrated ERS-2 SLC SAR imagettes using their research processor BSAR (Lehner et al., 2000).

The Canadian satellite RADARSAT-1 operates a ScanSAR with a frequency of 5.6 GHz, which transmits and receives horizontal (HH) polarization. In contrast to the ERS SAR it can image 500 km x 500 km areas with a resolution between 80 and 150 m depending on the utilized beam. Since February 1999 the images are radiometricaly calibrated for NRCS having a nominal radiometric accuracy of ±1.35 dB. In specific areas where scalloping occurs, an effect caused by an excessive large variation in the satellite yaw angle, calibration accuracy may be further degraded.

In contrast to the SAR the ERS-2 SCAT measures the backscatter from the ocean surface with three antennae. These beams continuously illuminate a 500 km wide swath with a resolution of 45 km and are co-located to the SAR imagettes. From these triplets the wind vectors with an accuracy of 1.2 ms^{-1} and 15° were derived by the Centre ERS d'Archivage et de Traitement (CERSAT), using the C-band model CMOD_IFR2 (Bentamy et al., 1994).

In addition to the ERS-2 SAR and SCAT data, co-located wind data from the atmospheric model of the European Centre for Medium-range Weather Forecast (ECMWF) were available. The model produced global ECMWF analysis wind fields for the four main synoptic hours 00, 06, 12 and 18 UTC and are available co-located to the SAR imagettes.

HIRLAM and REMO are state-of-the-art analysis and forecast systems for numerical weather forecasts. They are in operational use at several meteorological services, e.g., Danish Meteorological Institute. The high-resolution limited area model HIRLAM is a semi-implicit model, with Eulerian advection and leap frog time stepping. For the Greenland area it was set up with a time step of 240 s and a horizontal resolution of 0.5°. The analysis of the model is performed every 6 h using the optimum interpolation method. The lateral boundary values for the model are obtained from the global model of the European Center for Medium-range Weather Forecast (ECMWF). The Regional

Model (REMO) is a grid point model using the discretized primitive equations in a terrain-following hybrid coordinate system. The finite differencing scheme is energy preserving. The prognostic variables are surface air pressure, horizontal wind components, temperature, specific humidity and cloud water. A soil model is added to account for soil temperature and water content. For the here utilized 40 year run REMO is forced with reanalysis of the National Centers for Environmental Prediction (NCEP). REMO was setup with a horizontal resolution of 0.5°a time step of 5 min and a one hour output-interval.

3. Wind retrieval methods

SAR wind fields are retrieved in two steps. In the first step wind directions are retrieved, which are a necessary input in the second step to retrieve wind speeds. The SAR wind directions are retrieved from wind-induced phenomena that are visible in SAR images and which are aligned in wind direction. Wind induced streaks observed in SAR imagery are often interpreted as atmospheric boundary layer (ABL) rolls (Etling and Brown, 1993). However, several authors report that average SAR derived wind-row directions are within 15° of in situ surface wind directions with possible errors as large as 30° (Alpers and Brümmer, 1994; Vachon and Dobson, 1996; Fetterer et al., 1998; Lehner et al., 1998). This indicates that the considered features may not be induced by ABL rolls but other features such as streaks from foam or surfactants that are truly aligned with the surface wind.

The wind-induced phenomena are assumed to be approximately in line with the mean wind direction and are defined to be oriented normal to the local gradients derived from smoothed amplitude images. Therefore the SAR images are smoothed and reduced to a pixel size of 100, 200 and 400 m, representing scales between 200 and 1600 m. From these pixels the local directions are computed with a 180° ambiguity. The 180° ambiguity can be removed if wind shadowing is present, which is often visible in the lee of objects. If such features are not present in the image other sources, e.g., atmospheric models or in situ measurements, have to be considered.

For retrieving wind speeds from SAR data a model function relating the well calibrated NRCS of the ocean surface to the local near-surface wind speed, wind direction versus antenna look direction and incidence angle is applied. In general this function depends also on radar frequency and polarization. The CMOD4, which was developed for the scatterometer aboard ERS-1 (Stoffelen and Anderson, 1997), is the most commonly used function and has been applied successfully for wind speed retrieval from ERS-1 and ERS-2 SAR imagery (Vachon and Dobson, 1996; Fetterer et al., 1998; Lehner et al., 1998). For wind speed retrieval from C-band HH polarized SAR images no similar well developed model exists so that a hybrid model function is applied that consists of the CMOD4 and a C-band polarization ratio (PR)
(Horstmann et al., 2000a, 2000b; Thompson and Beal, 2000), defined as,

$$\mathrm{PR} = \frac{\sigma_0^{HH}}{\sigma_0^{VV}},$$

where σ_0^{HH} and σ_0^{VV} are the HH- and VV polarized NRCS, respectively. So far the PR is not well known and several different PRs are suggested in literature. In this paper the PR proposed by Thompson et al. (1998) is applied, which is given by:

$$\mathrm{PR} = \frac{(1+\alpha\tan^2\theta)^2}{(1+2\tan^2\theta)^2},$$

where θ is the incidence angle of the signal and α is a constant, which is set to 1 when utilizing RADARSAT-1 ScanSAR data processed in Gatineau at the Canadian Data Processing Facility (Horstmann et al., 2000b).

In case of the uncalibrated ERS-2 SLC SAR imagettes the CMOD4 model cannot be applied. Therefore a NN is applied, which is used as a multiple nonlinear regression technique to parameterize the relationship between the intensity measured by the SAR and ocean surface wind speed.

4. Global SAR wind retrieval

In contrast to the SAR image mode the SLC SAR imagettes are not calibrated for NRCS. Therefore a NN had to be trained to parameterize the dependency of the measured image intensity on the local wind (Horstmann et al., 2001). As a first step, an NN was trained to retrieve the wind speed from SAR imagettes considering only the mean imagette intensity. In Fig. 1 wind speeds from ECMWF and SCAT are plotted versus the wind speed resulting from SAR imagettes. Although wind direction was not considered, the statistics look quite good.

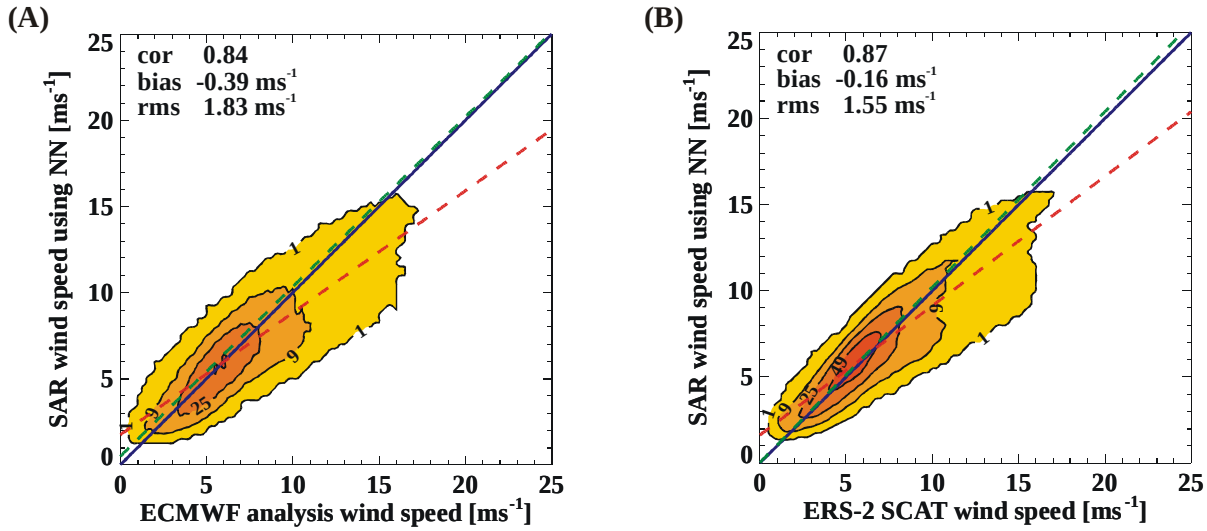

Figure 1: Scatterplot of ECMWF (A) and SCAT (B) wind speeds versus SAR-imagette retrieved wind speeds using a NN with SAR-imagette intensity as input.

To obtain a more accurate estimate of wind speed using a NN, wind direction was considered in addition to the mean SAR-imagette intensity. In Fig. 2 the ECMWF and SCAT wind speeds are plotted versus the co-located SAR-imagette-retrieved wind speeds. As anticipated the results are significantly better than without consideration of wind direction. Especially at wind speeds >10 ms^{-1} the dependence on wind direction leads to large errors. Comparison of wind speeds from SAR imagettes and SCAT shows the best consistency, which is expected, due to the similarity of the instruments.

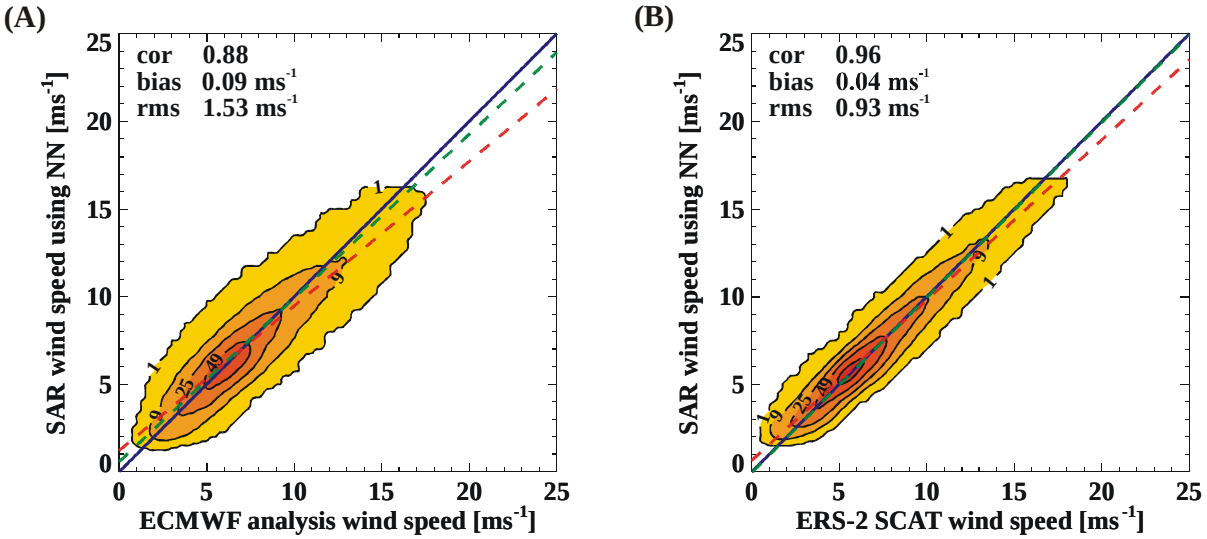

Figure 2: Scatterplot of ECMWF (A) and SCAT (B) wind speeds versus SAR-imagette retrieved wind speeds using a NN with SAR-imagette intensity as input.

5. Regional SAR wind retrieval

To show the applicability of the algorithms to ERS SAR images a comparison was performed to REMO results. Therefore 860 co-location were considered representing the results of 159 ERS-1 and ERS-2 SAR images. All utilized SAR images were acquired in the area of the North and Baltic Sea. Most of these SAR images were acquired at the coast or in its immediate neighborhood. Prior to SAR wind retrieval, all pixels representing land, sea ice and other artifacts not due to the wind were automatically masked. For comparison the SAR winds were retrieved on the same grid as the REMO model, representing a mean wind vector of an area of approximately 55 km x 55 km. The SAR and REMO results were co-located in time by interpolation of REMO. To remove the ambiguities in SAR wind direction retrieval wind shadowing was considered. In a few cases, were the ambiguities could not be removed using the SAR image information, weather charts were taken into account. In Fig. 3 the winds from REMO are plotted versus the SAR retrieved winds.

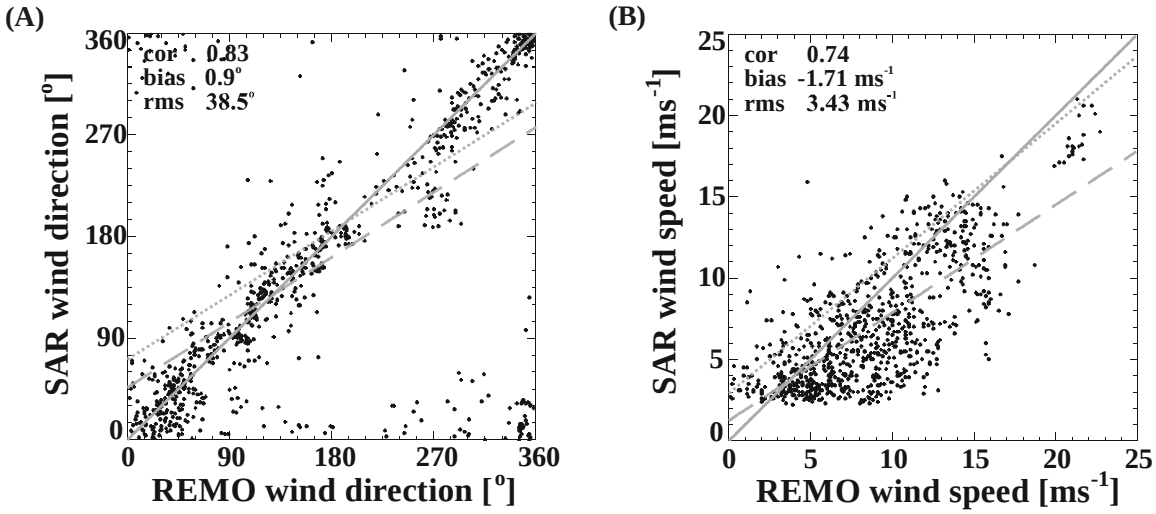

Figure 3: Scatterplot of comparison between REMO results and ESR SAR retrieved wind directions (A) and wind speeds (B).

The correlation for wind direction retrieval is 0.83 with a bias of 0.9° and a rms error of 38.4°. For wind speeds the correlation is 0.74 with a bias of 1.71 ms^{-1} and a rms error of 3.43 ms^{-1}. Both wind directions and wind speeds have a quit low correlation with a high rms error. Especially in case of wind speeds a much better agreement has been shown using the global set of ERS-SAR images (Section 4.). Most likely the differences in wind are due to the too coarse resolution of REMO, which was not setup to resolve the detailed coastal wind field. Especially in coastal regions the high variability of the wind field due to local topography is visible in SAR images. Unfortunately most of the considered SAR images were acquired at the coast or near to it so that much better coincidence cannot be expected.

To test the applicability of the wind retrieval algorithm on RADARSAT-1 ScanSAR data a comparison was performed considering 20 ScanSAR images in the area around the south tip of Greenland. All images were acquired at approximately 20:30 UTC and compared to the 21:00 UTC wind forecast of the HIRLAM model. ScanSAR wind vectors were retrieved from the area corresponding to the grid cell in the HIRLAM model, resulting in an average grid cell size of approximately 28 km x 55 km. Again all pixels representing land, sea ice and other artifacts not due to the wind were masked prior to wind retrieval. The directional ambiguities of the ScanSAR retrieved wind directions were removed by considering wind shadowing and the HIRLAM model. The resulting wind directions, mean NRCS's and mean incidence angles of each grid cell were taken as input to the algorithm.

The scatter plots of the comparison are shown in Fig. 4 The correlation for wind direction retrieval is 0.92 with a bias of -3.5°and a rms error of 21.6°. Wind directions can only be retrieved if wind streaks or shadowing are imaged, which are often missing at low wind speeds (<5 ms^{-1}). In addition, the loss of power in ScanSAR images, which occurs most significantly in near range due to saturation of the analogue to digital convertor (ADC) of the ScanSAR system \cite{HorstmannJ:00}, leads to a loss of modulation and therefore a loss of imaging of wind streaks. Furthermore, the HIRLAM model cannot resolve atmospheric fronts and coastal wind effects as well as the ScanSAR, due to its coarser resolution. This leads to a shift of fronts in time and space or even to their effacement.

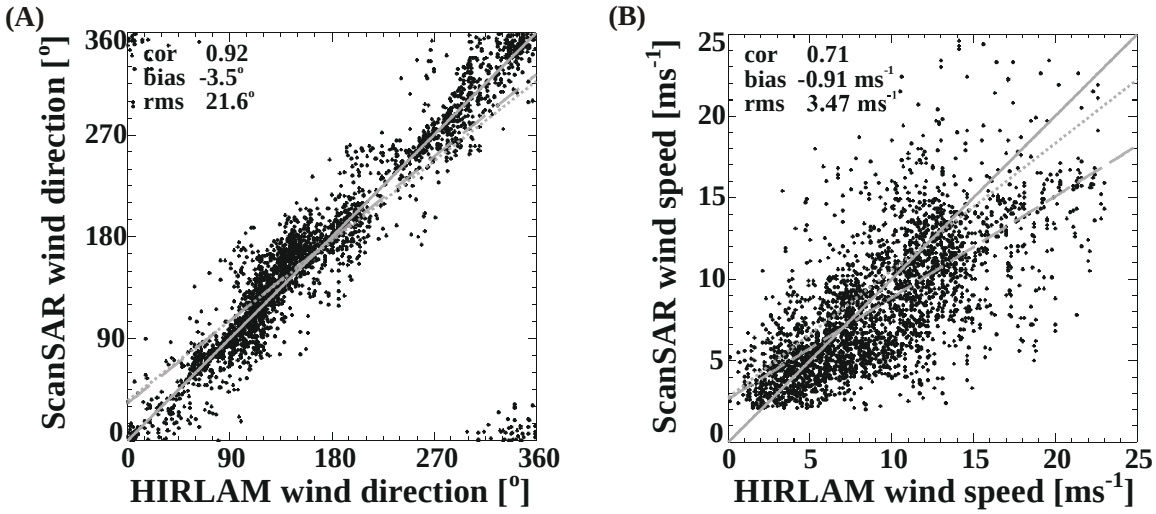

Figure 4: Scatterplot of comparison between HIRLAM model results and RADARSAT-1 ScanSAR retrieved wind directions (A) and wind speeds (B).

Comparison of wind speeds results in a correlation of 0.71 with a bias of -0.81 ms^{-1} and a rms of 3.47 ms^{-1}. The differences are mainly due to ADC saturation and differences in the lee of the coasts. Investigation of the dependency of the rms error and bias on incidence angle and wind speed showed a significant increase of rms error and decrease of bias for incidence angles below ~25°. This tendency is due to saturation of the ADC of the ScanSAR system, which causes an underestimation of wind speed. A strong change of rms error and bias was also observed at incidence angles between 39° and 45°, which can be explained by calibration inaccuracies of the corresponding beam W3.

6. Summary

An algorithm based on NN has been applied to parameterize the relation of uncalibrated SAR intensity measurements of the ocean surface to the local surface wind speed. The algorithm was applied to satellite borne SAR wave mode data of the European satellite ERS-2, which are available on a global and continuous basis. However, so far only 27 days of SAR wave mode data have been processed to SLC SAR imagettes, which are now available on a continuous basis from ENVISAT ASAR. Therefore the algorithms were especially tailored for the needs of ENVISAT ASAR and have been tested and validated using the ASAR like ERS-2 SLC SAR imagettes. Comparison of SAR derived wind speeds to ERS-2 SCAT measurements, under consideration of wind direction, resulted in a correlation of >0.95 and a rms error of ~1.0 ms^{-1}. If no wind direction information is available the correlation is 0.87 with an rms error of <2.0 ms^{-1}.

An further algorithm has been developed to retrieve mesoscale wind fields in coastal areas from well calibrated ERS-1, ERS-2 and RADARSAT-1 SAR data. In contrast to prior algorithms for wind direction retrieval, the algorithm computes both wind direction and wind speed in the spatial domain, and is therefore capable to derive the wind field near to the coast and exclude phenomenon’s not due

to the local wind e.g. ice and surface slicks. Comparison of SAR retrieved winds to numerical models resulted in case of ERS SAR in a correlation of 0.83 with a rms error of 38.4° for wind direction and 0.74 and 3.4 ms^{-1} for wind speed and in case of RADARSAT-1 ScanSAR in a correlation of 0.92 with a rms error of 21.6°for wind direction and 0.71 and 3.5 ms^{-1} for wind speed. The main differences in wind direction were identified at low wind speeds, near atmospheric fronts and the lee of the coasts. The first leads to the lack of imaging of wind induced streaks, which are needed for the wind direction retrieval while the other two are due to the too coarse resolution of the model in time and space. Main differences in wind speed were observed at low wind speeds and in the lee of the coast. In case of ScanSAR differences were also observed at low incidence angles (<30°) and in the range of 39° to 45° representing the ScanSAR beam W3, which are due to saturation of the ADC especially at low incidence angles and due to other calibration issues. Both calibration issues can be tackled and improved in future studies. Overall the results show the applicability of well calibrated SAR data for high resolution wind field retrieval especially in coastal areas.

Acknowledgments

The authors were supported by the German Bundesministerium für Bildung und Forschung in the framework of the project Environmental Oceanography (ENVOC). All ERS-1 and ERS-2 SAR images were provided by the Europena Space Agency. The RADARSAT-1 ScanSAR images were kindly made available by RADARSAT International.

References

Alpers, W., and Brümmer, B., (1994), Atmospheric Boundary Layer Rolls Observed by the Synthetic Aperture Radar Aboard the ERS-1 Satellite, *J. Geophys. Res.*, Vol. 99, pp. 12 613-12 621.

Etling, D., and Brown, R.A., (1993), Roll Vortices in the Planetary Boundary Layer: A Review, *Boundary-Layer Meteorol.*, Vol. 18, pp. 215-248.

Fetterer, F., Gineris, D., and Wackerman, C., (1998), Validating a scatterometer wind algorithm for ERS-1 SAR, *IEEE Trans. Geosci. Remote Sens.*, Vol. 36, No. 2, pp. 476-492.

Gerling, T.G., (1986), Structure of the surface wind field from Seasat SAR, *J. Geophys. Res.*, Vol. 91, pp.2 308-2 320.

Horstmann, J., Lehner, S., Koch, W., and Tonboe, R., (2000a), Computation of wind vectors over the ocean using spaceborne synthetic aperture radar, *John Hopkins APL Tech. Dig.*, Vol. 21, No. l, pp. 100-107.

Horstmann, J., Koch, W., Lehner, S., and Tonboe, R., (2000b), Wind retrieval over the ocean using synthetic aperture radar with C-band HH polarization, *IEEE Trans. Geosci. Remote Sens.*, Vol. 38, No. 5, pp. 2122-2131.

Horstmann, J., Lehner, S., and Schiller, H., (2001), Global wind speed retrieval from complex SAR data using scatterometer models and Neural Networks, *in Proc. Int. Geosci. Remote Sens. Symp.*, Sidney, Australia.

Horstmann, J., Koch, W., Lehner, S., and Tonboe, R., (2002), Ocean Winds fro RADARSAT-1 ScanSAR, *Can. J. Remote Sens.*, Vol. 28, No. 3, in press.

Koch, W., (2002), Directional Analysis of SAR Images Aiming at Wind Direction, *IEEE Trans. Geosci. Remote Sens.*, submitted.

Lehner, S., Horstmann, J., Koch, W., and Rosenthal, W., (1998), Mesoscale wind measurements using recalibrated ERS SAR images, *J. Geophys. Res.,* Vol. 103, pp. 7 847-7 856.

Lehner, S., J. Schulz-Stellenfleth, B. Schättler, H. Breit, and J. Horstmann, (2000), Wind and Wave Measurements using Complex ERS-2 SAR Wave Mode Data, *IEEE Trans. Geosci. Remote Sens.,* Vol. 38, No. *5,* pp. 2246-2257.

Stoffelen, A., and Anderson, D., (1997), Scatterometer data interpretation: Estimation and validation of the transfer function CMOD4, *J. Geophys. Res.,* Vol. 102, pp. 5 767-5 780.

Thompson, D.R., Elfouhaily, T.M., and Chapron, B., (1998), Polarization ratio for microwave backscattering from the ocean surface at low to moderate incidence angles, *in Proc. Int. Geosci. Remote Sens. Symp.* Seattle, USA.

Thompson, D.R., and Beal, R.C., (2000), Mapping of mesoscale and submesocale wind fields using synthetic aperture radar, *John Hopkins APL Tech. Dig.,* Vol. 21, No. 1, pp. 58-67.

Vachon, P.W., and Dobson, F.W., (1996), Validation of wind vector retrieval from ERS-1 SAR images over the ocean, *Global Atmos. Ocean Syst.,* Vol. 5, pp. 177-187.